The FASEB Journal express article 10.1096/fj.04-2421fje. Published online December 15, 2004.

Chemokine receptor CCR2 involvement in skeletal muscle regeneration

Gordon L. Warren,* Tracy Hulderman,[†] Dawn Mishra,[†] Xin Gao,[†] Lyndell Millecchia,[†] Laura O'Farrell,* William A. Kuziel,[‡] and Petia P. Simeonova[†]

*Department of Physical Therapy, Georgia State University, Atlanta, Georgia; [†]Health Effects Laboratory Division, National Institute for Occupational Safety and Health, Morgantown, West Virginia; [‡]Autoimmune and Inflammatory Diseases, Protein Design Labs, Fremont, California

*Corresponding author: Petia P. Simeonova, Health Effects Laboratory Division, National Institute for Occupational Safety and Health, Morgantown, West Virginia. E-mail: PSimeonova@cdc.gov

ABSTRACT

Chemokines, signaling through the CCR2 receptor, are highly expressed in injured skeletal muscle. Their target specificity depends on the cellular expression of the specific receptors. Here we demonstrate that, in freeze-injured muscle, CCR2 co-localized with Mac-3, a marker of activated macrophages as well as with myogenin, a marker of activated muscle precursor cells. The degeneration/regeneration process in skeletal muscle of CCR2–/– and wild-type mice was not significantly different at day 3. However in contrast to the regenerated muscle of the wild-type mice, the muscle from CCR2–/– mice was characterized by impaired regeneration, inflammation, and fibrotic response at day 14, increased fat infiltration, fibrosis, and calcification at day 21, and impaired strength recovery until at least 28 days post-injury. Consistently, the increased expression of Mac-1 and TNF-α was prolonged in the injured muscle of CCR2–/– mice. The expression pattern of the myogenic factors MyoD and myogenin was similar for both types of mice, while NCAM, which is associated with the initiation of fusion of muscle precursor cells, was more increased in the injured muscle of CCR2–/– mice. In conclusion, the study delineates that signaling through CCR2 is involved in muscle precursor cell activities necessary for complete and rapid regeneration of injured skeletal muscle.

Key words: skeletal muscle injury • inflammation • myogenesis • adipogenesis • CCL2

Skeletal muscle has the ability to regenerate itself in response to injury. The processes by which regeneration occurs are attributed to a small population of cells resident in adult skeletal muscle, referred to as satellite cells or muscle precursor cells (1, 2). Upon activation following muscle damage, muscle precursor cells migrate to the injured site and initiate regeneration. The influx of inflammatory cells, principally monocytes/macrophages, while originally thought to be responsible only for phagocytosis of necrotic myofibers, is now considered an essential event for controlling all aspects of muscle regeneration. Increasing evidence has demonstrated that cytokines and growth factors released by activated macrophages,

such as hepatocyte growth factor (HGF), insulin-like growth factor (IGF), fibroblast growth factor (FGF), and tumor necrosis factor (TNF) α, modulate muscle precursor cell behavior during muscle regeneration and contribute to the functional recovery after injury (1, 3–6). If the regeneration process is compromised or insufficient, muscle tissue may be replaced by scar tissue which is typically associated with an impaired functional capacity (7).

Recently we demonstrated that monocyte chemoattractant protein-1 (MCP-1;CCL2) and its receptor CCR2 are expressed in the injured skeletal muscle (8, 9). Furthermore, if the MCP-1-CCR2 axis is suppressed by genetic modulation or immune neutralization, muscle functional restoration after injury is delayed (9). Although, the MCP-1-CCR2 role is thought to be primarily that of modulating the migration of mononuclear leukocytes into the site of inflammation, this pathway has been shown to affect migratory and proliferative activities in non-hematopoietic cells such as endothelial, smooth muscle, and mesothelial cells (10, 11). We hypothesized that signaling through CCR2 can regulate muscle precursor cells as well as macrophages in the process of muscle regeneration. To test this hypothesis, we characterized the localization of CCR2 in regenerating muscle (freeze-injured mouse tibialis anterior [TA] muscle) and compared the cellular and molecular characteristics of skeletal muscle regeneration in CCR2 deficient (–/–) vs. wild-type mice. Our data suggest that muscle precursor cells as well as macrophages express the CCR2 receptor and that signaling through this receptor is involved in skeletal muscle regeneration after injury.

MATERIALS AND METHODS

Animals

CCR2–/– mice on a mixed C57BL/6 × strain 129 genetic background were generated as described previously (12, 13). The CCR2–/– mice were then backcrossed to C57BL/6 mice for 10 generations. C57BL/6J mice were obtained from the Jackson Laboratory. Ages for all mice were between 18 and 24 weeks. The mice were provided food and water ad libitum and were maintained on a 12–h light/dark cycle. In preparation for muscle injury induction, most mice were anesthetized with 0.33 mg/kg fentanyl, 16.7 mg/kg droperidol, and 5.0 mg/kg diazepam administered i.p. In experiments assessing muscle strength both before and following injury, mice were induced and maintained on isoflurane anesthesia during the injury induction and strength-testing procedures. Animal care and use procedures, including death by CO_2 asphyxiation, were conducted in accordance with criteria outlined in the “PHS Policy on Humane Care and Use of Laboratory Animals” and the “Guide for the Care and Use of Laboratory Animals” (NIH Publication 86-23, 1996); these procedures were approved by the Georgia State University and NIOSH institutional animal care and use committees.

Induction of freeze-induced muscle injury

The procedure used was identical to that described previously (5). In brief, a 1.5-cm-long incision was made through aseptically prepared skin overlying the left TA muscle belly. Injury was induced by applying a steel probe cooled to the temperature of dry ice to the TA muscle belly for 10 s. The skin incision was then closed using silk suture.

Measurement of in vivo muscle strength

For assessing the functional recovery from injury, mice were implanted with a chronic stimulating nerve cuff placed on the left common peroneal nerve as described previously (14). Briefly, the nerve cuff was constructed from two Teflon-coated, multi-stranded 90% platinum: 10% iridium wires (0.15 mm). An incision was made through the biceps femoris muscle, and the two loops, formed from 2.5 mm segments of de-insulated platinum:iridium wire, were placed around the common peroneal nerve. The proximal end of the nerve cuff was externalized in the dorsal cervical region where it could be connected to a stimulator. Mice implanted with nerve cuffs were allowed 4–6 weeks to recover before being used in the experiments. Isometric tetanic torque of the left anterior crural muscles was measured using a miniature dynamometer as described previously (14). Using 200 ms trains of 0.1 ms pulses at 300 Hz, stimulation voltage was adjusted to yield the maximal isometric tetanic torque of the anterior crural muscles. Muscle strength was measured immediately before and after injury and at 3, 7, 14, 21, and 28 days post-injury.

Real-time RT-PCR

TA muscles were collected in RNAlater® (Qiagen, Valencia, CA), homogenized and total RNA extracted using a commercial kit (RNeasy, Qiagen) following the manufacturer's protocol. cDNA was synthesized from 1 μg of RNA using Superscript II® (Life Technologies, Gaithersburg, MD). Real-time PCR for TNF-α and 18S/rRNA were performed using pre-developed primers and probes (TaqMan assay reagents®, PE Applied Biosystems, Foster City, CA) on an ABI Prism 7700 Sequence detector (PE Applied Biosystems). For some mRNAs, amplification reactions were performed with 1 × SYBR® Green PCR master mix (PE Applied Biosystems), 1 μM primers, and 4 μl of cDNA in a 50 μl final volume with the following designed primers (Invitrogen Life Technologies, Carlsbad, CA): Mac1 forward (F): GAT GAG ACA AAG AAC AAC ACA C reverse (R):TGA AGA ACC TCT GAG CAT CC; Myogenin (F): GCA CTG GAG TTC GGT CCC AA (R):TAT CCT CCA CCG TGA TGC TG; Myo-D (F): ACC CAG GAA CTG GGA TAT GGA (R): AAG TCG TCT GCT GTC TCA AA; NCAM (F): ACG GCC ATG GAA CTA GAG GA (R): TCC GGA GGC TTC ACA GGT C; 28S/rRNA (F): GAA GGC AAG ATG GGT CAC CA (R): GAA CTT CCG TGG GTG ACT CC.

The comparative threshold cycle (C_T) method was used to calculate the relative concentrations. This method involved obtaining C_T values for the transcript of interest, normalizing to the housekeeping gene 18S (28S)/rRNA and comparing the relative increases between control and experimental samples.

Histopathology

All histopathological and immunohistological evaluations were conducted on at least 4 mice per group. For cross-section histology and immunohistology, muscles were embedded in Tissue Tek OCT (Miles Scientific), frozen in isopentane, and stored at –80°C. Using a microtome cryostat at –20°C, 10 cross sections (10 μm thick) were cut at each of 6 levels equally spaced along the length of the TA muscle. Sections at each level were stained for routine H&E or used for immunohistology. Myofiber cross-sectional areas (CSA) in regenerating muscles were determined by using H&E-stained sections. Sections chosen for analysis those with 1) the

highest fraction of the muscle area showing injury/regeneration; 2) a well-demarcated border between the regions of regenerating and uninjured myofibers; only fibers in the vicinity of the border were analyzed. Regenerating myofibers chosen for analysis were centronucleated fibers not bordering a fiber that was not centronucleated. Likewise, uninjured myofibers chosen for analysis were non-centronucleated fibers that did not border a centronucleated fiber. Between 202 and 434 myofibers were analyzed per muscle. For each muscle, the average uninjured and regenerating myofiber areas were determined by using at least five mice per group. Measurements were performed using a Leica Leitz DMRB microscope, ×20 objective, and MediaCybernetics Optimas 6.5 software (Media Cybernics, Silver Spring, MD).

Muscles processed for longitudinal-section histology were fixed by immersion in 10% neutral-buffered formalin. Fixed tissues were embedded in paraffin, cut into 6-μm longitudinal sections, and stained with hematoxylin-eosin (H&E) for blinded histopathological assessment. Masson's trichrome stain and Van Kossa's stain to visualize collagen and calcium deposits, respectively, were applied as described originally (15). The histopathology was graded independently by 2 researchers using a 1-to-5 scale (1=minimal histopathology; 2=slight/mild; 3=moderate; 4=moderately severe; 5=severe/high) and at least 3 mice per group.

Specific rat anti-mouse monoclonal antibodies for Mac-3, Gr-1 (BD PharMingen, San Diego, CA), NCAM (Chemicon International, Temecula, CA), CD31 (Abcam, Cambridge, UK), and ER-TR7 (Acris, Hiddenhausen, Germany) were applied in an immunostaining protocol conducted on acetone-fixed cross-cryosections as described before (5). The positive staining was evaluated visually by two independent researchers and quantitatively by Optimas image analysis software, version 6.51. Images of stained sections (two regions of the injured portion of each muscle section, 2 sections per animal, 4 animals per group, ×20 magnification) obtained with Leica DMRB microscope and captured by a Sony DXC9000 color video camera were used for the image analysis. After we set red, green, and blue thresholds to estimate the stained areas, the Optimas software measured the total area, stained area, and percent stained area. The same thresholds and lighting conditions were used for all sections for a given stain.

Immunostaining for CCR2, myogenin, and desmin was performed on formalin-fixed cross-cryosections using specific polyclonal antibodies prepared in goats (Santa Cruz Biotechnology, Santa Cruz, CA). The antibodies were diluted 1:300 in phosphate-buffered saline (PBS) and applied to the sections for 1 h at RT. Binding of the primary antibodies was visualized using the ImmunoCruz staining system (Santa Cruz Biotechnology) and Tyramide Signal amplification kit (Molecular Probes, Eugene, OR) according to the manufacturers' instructions. For other immunofluorescence staining, specific secondary antibodies conjugated with Cy^{TM}3 or Fluorescein (FITC) (Jackson Immunoresearch Labs, Weston Grove, PA) were used in concentrations suggested by the manufacturer. Mounting media containing DAPI was used for nuclear localization. A Zeiss LSM 510 laser confocal microscope (Carl Zeiss Inc., Thornwood, NY) was used to obtain images. Laser lines at 364, 488, and/or 543 nm were used depending on the fluorophore(s) in use. Control experiments without primary antibody demonstrated that immunostaining signals observed were specific.

Statistics

Differences in mRNA transcript levels between the two groups of mice were analyzed using unpaired *t*-tests or Mann-Whitney tests when assumptions of normality or equal variance were violated; Bonferroni adjustments were applied to control for Type I error inflation due to the multiple comparisons.

For comparison of myofiber CSAs between the two groups of mice, first an average CSA for each type myofibers (regenerating or uninjured) in each muscle was calculated. These averaged CSA values were then analyzed using the two-way (group × myofiber type) repeated measures ANOVA. For immunostaining comparison, the percent stained area was averaged for each muscle and analyzed by ANOVA single factor.

Strength differences between the two groups of mice were analyzed using the two-way (group × time) repeated measures ANOVA. When significant interactions were found, single degree-of-freedom contrasts were applied as post hoc tests. All statistical testing was conducted using SPSS (version 10.0). An α-level of 0.05 was used for all analyses. Values presented in the Results are means ± SE.

RESULTS

CCR2 cellular localization in injured skeletal muscle

We have previously demonstrated that MCP-1 as well as CCR2 proteins are not expressed in control (uninjured) TA muscle but injury induces their expression (9). To determine whether the expression of CCR2 is localized to macrophages and/or muscle precursor cells in injured muscle, we conducted double immunostaining for CCR2 and Mac-3, a marker of activated monocytes/macrophages (16) or myogenin, a marker of activated and differentiating muscle precursor cells (1, 2). Similar to our previous observations (5), a considerable number of Mac-3 positive cells and myoblasts expressing myogenin were observed in the damaged muscle area by 2 days post-injury. CCR2 was found to be localized to the plasma membrane of cells expressing cytoplasmic-localized Mac-3 (Fig. 1*A*) or nuclear-localized myogenin (Fig. 1*B*), demonstrating that both macrophages and muscle precursor cells are targets for MCP-1 signaling.

CCR2–/– mice show a regeneration defect with enhanced adipogenesis and fibrosis

To evaluate the role of CCR2 in muscle regeneration we compared CCR2–/– and wild-type mice on the histological characteristics of TA muscle regeneration after freeze injury. Analysis of H&E-stained sections demonstrated no visible differences between the two types of mice regarding the histology of control TA muscle (data not shown) as well as in the extent of tissue damage and inflammatory response observed at 3 days post-injury (Fig. 2*A*). Two weeks after injury, virtually no sign of previous damage, except for regenerated myofibers with centrally located nuclei, was detectable in wild-type mice, indicating a complete regeneration (Fig. 2*B*). However, in CCR2–/– mice the picture was different, including increased interstitial space, high numbers of inflammatory cells, large rounded (swollen) myofibers, and small centrally nucleated myofibers, demonstrating an impaired regeneration (Fig. 2*B*). To quantify the impaired regeneration in the CCR2–/– mice, we compared the regenerating myofiber CSA at day 14 post-

injury in 7 CCR2–/– mice to that measured in 5 wild-type mice. As presented in Fig. 2*C*, the mean regenerating myofiber CSA was 60% smaller in the CCR2–/– mice compared with that in the wild-type, whereas no significant difference was found between the two types of mice in the CSA of uninjured myofibers. To evaluate whether the enlarged interstitial space in the injured muscle from CCR2–/– mice was associated with fibroblast accumulation, we conducted immunostaining for ER-TR7, a marker of reticular fibroblasts (17). At 14 days after injury, positive staining was found to surround the regenerated myofibers in wild-type mice (9.3±2.57% stained area, n=4), but the staining was expanded markedly in the interstitial space of injured muscles from the CCR2–/– mice (45.3±5.8% stained area, n=4, P<0.05; Fig. 2*D*). Three weeks after injury, histopathological abnormalities were no longer noticeable in the muscle from wild-type mice (Fig. 2*E*). In contrast, fat infiltration was apparent in the injured muscle of CCR2–/– mice as shown by H&E-staining (Fig. 2*E*). Collagen, as demonstrated by blue staining in Masson's trichrome-stained sections, was distributed around the fat deposits in the injured muscles of CCR2–/– mice (Fig. 2*F*). Furthermore, the fibrosis was accompanied by calcium deposition in the injured muscles of CCR2–/– mice (Fig. 2*G*). Histopathological grading of the fat infiltration, fibrosis, and calcium deposition at 21 days post-injury averaged a 3 (moderate to severe extent) in the CCR2–/– mice compared with a 1 (minimal alterations) in the wild-type mice (Table 1).

Modified inflammatory response occurs in injured skeletal muscle of CCR2–/– mice

The inflammatory response was evaluated by immunostaining for Mac-1 (integrin β 2 subunit, CD18 β subunit), a marker of leukocytes, including monocytes/macrophages and neutrophils or, more specifically, by Mac-3, a marker of monocytes/macrophages (16), and Gr-1, a marker of neutrophils (18). At 3 days after injury, the infiltrating inflammatory cells in the damaged muscle regions from both types of mice C57BL/6 and CCR2–/– were positive for Mac-1 (data not shown) and Mac-3 (Fig. 3*A*). The number of monocytes/macrophages that accumulated in the injured muscle was not visibly reduced in CCR2–/– compared with the wild-type mice. The quantification of staining for Mac-1 or Mac-3 demonstrated around 30% staining area in the WT as well as the CCR2–/– injured muscles. At 14 days after injury, while the injured muscles of wild-type mice showed minimal Mac-1 or Mac-3 immunostaining (8.6±2.5% stained area, n=4) those of CCR2–/– mice were characterized with extensive immunostaining (37.56±3.11 % stained area, n=4, P<0.05), indicating a prolonged period of macrophage accumulation (Fig. 3*C*). There was minimal Gr-1 immunostaining at 3 days after injury in muscles from both types of mice (Fig. 3*B*), and no staining was present in either type at 14 days post-injury.

Since it has been suggested that chemokines play a role in angiogenesis, immunohistochemistry for a vascular endothelial cell marker, CD31/PECAM-1 (19), was conducted to assess whether angiogenesis was impaired in regenerating muscle of CCR2–/– mice. We observed no differences in the number of CD31-positive cells between the CCR2–/– and wild-type groups (Fig. 3*D*). However, we cannot rule out the possibility that small differences in the number or diameter of microvessels may exist between the CCR2–/– and wild-type mice.

For semi-quantification of the inflammatory response in injured muscle, expression of genes coding for inflammatory markers or mediators was evaluated by real-time PCR. The temporal expression of the inflammatory cell marker, Mac-1, was consistent with the histological and immunohistological evaluation of the inflammatory response. Mac-1 expression was increased

by injury but no significant difference was found between the CCR2–/– and the wild-type mice at 1 or 3 days after injury. At 14 days after injury, Mac-1 expression had dropped to control levels in the wild-type mice, but expression remained elevated in the CCR2–/– mice (Fig. 4*A*). Furthermore the inflammatory response was quantified by the expression of TNF-α, a major pro-inflammatory mediator associated with monocyte/macrophage accumulation in the injured muscle (5). The largest increase in the expression of TNF-α occurred within 24 h of injury in both types of mice (Fig. 4*B*). The rapid increase in TNF-α mRNA transcript levels was followed by a gradual reduction over the first three days post-injury and a return to control levels by day 14 in the wild-type mice. In contrast, the reduction in TNF-α expression was delayed in the CCR2–/– mice as expression at 3 days after injury was significantly higher compared with the wild-type mice, and expression remained above control levels even at 14 days post-injury (Fig. 4*B*).

Myogenesis and muscle functional recovery post-injury are altered in CCR2–/– mice

To evaluate the extent of activation and maturation of muscle precursor cells, real-time PCR was used to determine the expression of MyoD, myogenin, and NCAM, markers of proliferating, differentiating, and fusing muscle precursor cells, respectively (1, 2). Myogenin expression was increased by injury to the same extent in muscles of wild-type and CCR2–/– mice at 1, 3, and 14 days post injury (Fig. 5*A*). Similarly, no difference between the two types of mice was observed in the expression of MyoD (Fig. 5*B*). In contrast, at 3 and 14 days post-injury, real-time PCR demonstrated greater NCAM mRNA transcript levels in muscles of CCR2 –/– mice compared with those of wild-type mice (Fig. 5*C*). To analyze whether the difference in gene expression was manifested at the protein level, immunostaining was conducted. As we previously reported, cells with MyoD and myogenin immunostained nuclei were spread in the injured area of the C57BL/6 TA muscle 3 days (high intensity of the color) and 14 days (lower intensity of the color) post-injury (Gordon, 2002). The findings from MyoD and myogenin immunostaining, consistent with the real-time PCR results, were not different between C57BL/6 and CCR2–/– mice. Consistent with the RT-PCR findings again, NCAM protein levels were increased in the injured muscle of CCR2–/– mice compared with wild-type mice at 3 days post-injury (0.7±0.2 vs 11.6±3% stained area, respectively; n=4, P<0.05; Fig. 6*A*). Furthermore, at 14 days post injury, in contrast to the minimal NCAM immunostaining observed in some centronucleated myofibers of wild-type injured muscle (3.7±2 % stained area, n=4), strong positive immunostaining of small centronucleated cells was observed in the injured muscle of CCR2–/– mice (58.2±8.5 % stained area, n=4, P<0.05; Fig. 6*B*). Normal serum, used as a negative control, did not show any non-specific tissue staining (Fig. 6*C*). Since NCAM expression is not unique to regenerating muscle cells, immunostaining for desmin was performed on serial sections to determine whether the cells expressing NCAM were myoblasts and/or myotubes. The positive immunostaining for NCAM coincided with positive staining for desmin (Fig. 7).

To evaluate whether histological and molecular differences between the regenerating muscles from C57BL/6 and CCR2–/– mice are associated with a difference in the course of functional recovery from injury, maximal isometric torque production of the anterior crural muscles was measured before and at several time points after injury (Fig. 8). Both types of mice (n=7 each) demonstrated similar muscle strengths prior to injury as well as similar decrements immediately after injury (i.e., 59%). However, recovery of strength was apparent in the wild-type mice by 7 days post-injury but not in the CCR2–/– mice (P=0.008). The slower rate of strength recovery

for the CCR2–/– mice was maintained during the second week of recovery. By 14 days post-injury, the strength deficits for the wild-type and CCR2–/– mice were 28 and 42%, respectively, (P=0.001). This between-group difference in strength deficit was maintained until at least 28 days post-injury.

DISCUSSION

In the current studies, we demonstrated that a deficiency of CCR2 leads to histopathological as well as functional impairments during skeletal muscle regeneration after experimentally induced injury. A delay in the regenerative process was accompanied with prolonged inflammation, increased fat accumulation and a fibrotic response in the injured skeletal muscle of CCR2–/– mice. These alterations may be related to impaired activities of macrophages and/or muscle precursor cells, both of which express the CCR2 receptor following injury. Although this study suggests for the first time that CCR2-dependent signals are involved in regulation of muscle precursor cells in muscle regeneration, a role for CCR2 in noninflammatory cells and processes is not surprising since it has been shown that the MCP-1-CCR2 axis participates in processes such as angiogenesis and re-epithelization (10, 20, 21). The genetic deficiency of CCR2 led to more severe effects on skeletal muscle regeneration and fibrosis compared with the immunological MCP-1 neutralization applied in our early studies (9). The discrepancy might be related to incomplete MCP-1 neutralization by the immune approach, contribution of other chemokines that signal through CCR2, such as MCP-2 and -5 (22, 23), and ligand-independent CCR2 signaling.

Monocytes/macrophages in the freeze-injured skeletal muscle express CCR2, but CCR2 deficiency, as well as MCP-1 neutralization reported earlier (9), does not lead to a drastic reduction in the monocyte/macrophage influx or a shift toward a neutrophil-dominated inflammatory response. In our injury model, signaling through the CCR2 receptor is probably involved in activation of monocytes/macrophages, since the duration of macrophage infiltration and presence of degenerating myofibers was prolonged in the injured CCR2–/– muscle. Consistent with our findings, it has been demonstrated that the dermal healing in MCP-1 deficient mice is delayed but the influx of mononuclear cells is not affected (24). Other models of acute inflammation have demonstrated a significantly reduced influx of mononuclear cells in MCP-1 or CCR2 deficient mice. For example, it has been demonstrated that this chemokine deficiency is associated with an impaired thioglycolate-elicited peritoneal inflammation (12) and a reduced inflammation in the injured peripheral nervous system (25). Thus, the monocyte/macrophage influx may be modulated by MCP-1-CCR2 in a tissue- and/or injury-specific manner. Furthermore, the increased expression of TNF-α, a major pro-inflammatory mediator released mostly by the macrophages, was slower to return to baseline levels in injured muscles from CCR2–/– mice. This prolonged, elevated TNF-α response may play a role in the development of fibrosis in the injured CCR2–/– muscle. TNF-α has been shown to accelerate fibrogenesis in inflammatory liver and heart models in the mouse (26, 27).

The recovery of muscle strength, a reliable indicator of muscle function, was significantly delayed after injury in CCR2–/– mice compared with wild-type mice. The slower recovery of strength in the CCR2–/– mice is presumably due to slower rate of degeneration/regeneration processes occurring in those mice. Although there is a marked increase in fat and fibrosis in CCR2–/– injured muscle compared with the WT, it is doubtful that the difference in strength

recovery between the two groups of mice can be explained by that, since these histopathological findings represent ~5% of the muscle volume. Muscle precursor cells are considered to play an obligatory role in muscle regeneration as well as the recovery of strength, probably by assisting in the restoration of contractile protein and nuclear content (28). After activation, resident muscle precursor cells replicate and migrate from surrounding uninjured areas to the injured site where they fuse together to form myotubes, which mature into normal-sized myofibers (1, 29). In addition, a small proportion of the muscle precursor cells may originate from bone-marrow precursors, which migrate to the injured area of the muscle (30). The high gradient of MCP-1 in injured muscle might direct the migration of muscle precursor cells expressing CCR2. The replication and differentiation processes of the muscle precursor cells are probably not dependent on signaling through the CCR2 receptor since gene expression of the myogenic regulatory factors MyoD and myogenin was not significantly affected by the CCR2 deficiency. NCAM, also expressed on activated muscle precursor cells, has been associated with their fusion and maturation (31, 32). The altered temporal pattern of NCAM expression by muscle precursor cells in injured CCR2–/– muscle might be a compensatory response to impaired fusion activities of CCR2 deficient cells. Our observation of smaller regenerating myofibers 2 weeks after injury in the CCR2–/– mice compared with wild-type mice supports a possible role for CCR2 in modulating myoblast fusion processes during regeneration. During the course of maturation, myoblasts fuse to each other to form syncytial myofibers. This process includes multiple steps, including cell migration, alignment, recognition, adhesion, and membrane fusion (33). Although the controlling mechanisms for fusion are not well understood, it has been demonstrated that the immune mediator IL-4, through induction of calcium-dependent cell signals, may act as a myoblast recruitment factor facilitating the formation of myotubes (34). Similarly to the IL-4 signaling pathway, the dimerization of CCR2, induced for example by ligand binding, uses JAK-STAT (Janus kinase/signaling transducer and activator of transcription) activation followed by Gi-mediated Ca^{2+} intracellular flux (35, 36). Thus through these pathways, CCR2 activation in muscle precursor cells may contribute to the migratory and fusion processes occurring during muscle regeneration. In addition to the impaired myogenesis in CCR2–/– mice, an increased deposition of adipose tissue was observed in regenerating CCR2–/– muscle. We previously made similar observations in injured muscles of mice that were immune-neutralized for MCP-1 (9). A replacement of muscle mass by adipose cells is seen in Duchenne muscular dystrophy and in mice carrying targeted disruptions of the myogenic bHLH proteins (37, 38). The switch from myoblasts to adipocytes has been related to the expression of key adipogenic factors, such as PPARγ and C/EBPα (39). It is possible that the MCP-1-CCR2 signaling axis directly modulates adipogenesis or that the fat deposition occurs as a compensatory event for the impaired myogenesis. Future in vitro studies would clarify CCR2's role in myoblast migration, fusion and adipogenesis.

Overall, the data from the present study indicate that CCR2 is required in certain pathophysiological conditions, including skeletal muscle injury for complete regeneration. Understanding the role of CCR2 and its ligands in the mechanisms of muscle regeneration may help in development of therapeutics for speeding recovery of muscle injury and/or atrophy as well as in optimization of the protocols for healing of infarcted myocardium through myoblast transplantation.

REFERENCES

1. Hawke, T. J., and Garry, D. J. (2001) Myogenic satellite cells: physiology to molecular biology. *J. Appl. Physiol.* **91,** 534–551

2. Seale, P., Asakura, A., and Rudnicki, M. A. (2001) The potential of muscle stem cells. *Dev. Cell* **1,** 333–342

3. Winn, N., Paul, A., Musaro, A., and Rosenthal, N. (2002) Insulin-like growth factor isoforms in skeletal muscle aging, regeneration, and disease. *Cold Spring Harb. Symp. Quant. Biol.* **67,** 507–518

4. Floss, T., Arnold, H. H., and Braun, T. (1997) A role for FGF-6 in skeletal muscle regeneration. *Genes Dev.* **11,** 2040–2051

5. Warren, G. L., Hulderman, T., Jensen, N., McKinstry, M., Mishra, M., Luster, M. I., and Simeonova, P. P. (2002) Physiological role of tumor necrosis factor a in traumatic muscle injury. *FASEB J.* **0,** 201871–201111

6. St Pierre, B. A., and Tidball, J. G. (1994) Macrophage activation and muscle remodeling at myotendinous junctions after modifications in muscle loading. *Am. J. Pathol.* **145,** 1463–1471

7. Huard, J., Li, Y., and Fu, F. H. (2002) Muscle injuries and repair: current trends in research. *J. Bone Joint Surg. Am.* **84-A,** 822–832

8. Summan, M., McKinstry, M., Warren, G. L., Hulderman, T., Mishra, D., Brumbaugh, K., Luster, M. I., and Simeonova, P. P. (2003) Inflammatory mediators and skeletal muscle injury: a DNA microarray analysis. *J. Interferon Cytokine Res.* **23,** 237–245

9. Warren, G. L., O'Farrell, L., Summan, M., Hulderman, T., Mishra, D., Luster, M. I., Kuziel, W. A., and Simeonova, P. P. (2004) Role of CC chemokines in skeletal muscle functional restoration after injury. *Am. J. Physiol. Cell Physiol.* **286,** C1031–C1036

10. Nasreen, N., Mohammed, K. A., Galffy, G., Ward, M. J., and Antony, V. B. (2000) MCP-1 in pleural injury: CCR2 mediates haptotaxis of pleural mesothelial cells. *Am. J. Physiol. Lung Cell. Mol. Physiol.* **278,** L591–L598

11. Denger, S., Jahn, L., Wende, P., Watson, L., Gerber, S. H., Kubler, W., and Kreuzer, J. (1999) Expression of monocyte chemoattractant protein-1 cDNA in vascular smooth muscle cells: induction of the synthetic phenotype: a possible clue to SMC differentiation in the process of atherogenesis. *Atherosclerosis* **144,** 15–23

12. Kuziel, W. A., Morgan, S. J., Dawson, T. C., Griffin, S., Smithies, O., Ley, K., and Maeda, N. (1997) Severe reduction in leukocyte adhesion and monocyte extravasation in mice deficient in CC chemokine receptor 2. *Proc. Natl. Acad. Sci. USA* **94,** 12053–12058

13. Kuziel, W. A., Dawson, T. C., Quinones, M., Garavito, E., Chenaux, G., Ahuja, S. S., Reddick, R. L., and Maeda, N. (2003) CCR5 deficiency is not protective in the early stages of atherogenesis in apoE knockout mice. *Atherosclerosis* **167,** 25–32

14. Warren, G. L., Ingalls, C. P., and Armstrong, R. B. (1998) A stimulating nerve cuff for chronic in vivo measurements of torque produced about the ankle in the mouse. *J. Appl. Physiol.* **84,** 2171–2176

15. Sheehan, D., and Hrapchak, B. (1980) *Theory and Practice of Histotechnology.* Battelle Press, Ohio

16. Ralph, P., Ho, M. K., Litcofsky, P. B., and Springer, T. A. (1983) Expression and induction in vitro of macrophage differentiation antigens on murine cell lines. *J. Immunol.* **130,** 108–114

17. Van Vliet, E., Melis, M., Foidart, J. M., and Van Ewijk, W. (1986) Reticular fibroblasts in peripheral lymphoid organs identified by a monoclonal antibody. *J. Histochem. Cytochem.* **34,** 883–890

18. Cooper, K. D., Duraiswamy, N., Hammerberg, C., Allen, E., Kimbrough-Green, C., Dillon, W., and Thomas, D. (1993) Neutrophils, differentiated macrophages, and monocyte/macrophage antigen presenting cells infiltrate murine epidermis after UV injury. *J. Invest. Dermatol.* **101,** 155–163

19. Piali, L., Hammel, P., Uherek, C., Bachmann, F., Gisler, R. H., Dunon, D., and Imhof, B. A. (1995) CD31/PECAM-1 is a ligand for alpha v beta 3 integrin involved in adhesion of leukocytes to endothelium. *J. Cell Biol.* **130,** 451–460

20. Weber, K. S., Nelson, P. J., Grone, H. J., and Weber, C. (1999) Expression of CCR2 by endothelial cells: implications for MCP-1 mediated wound injury repair and In vivo inflammatory activation of endothelium. *Arterioscler. Thromb. Vasc. Biol.* **19,** 2085–2093

21. Kunkel, S. L. (1999) Through the looking glass: the diverse in vivo activities of chemokines. *J. Clin. Invest.* **104,** 1333–1334

22. Sarafi, M. N., Garcia-Zepeda, E. A., MacLean, J. A., Charo, I. F., and Luster, A. D. (1997) Murine monocyte chemoattractant protein (MCP)-5: a novel CC chemokine that is a structural and functional homologue of human MCP-1. *J. Exp. Med.* **185,** 99–109

23. Vande Broek, I., Asosingh, K., Vanderkerken, K., Straetmans, N., Van Camp, B., and Van Riet, I. (2003) Chemokine receptor CCR2 is expressed by human multiple myeloma cells and mediates migration to bone marrow stromal cell-produced monocyte chemotactic proteins MCP-1, -2 and -3. *Br. J. Cancer* **88,** 855–862

24. Low, Q. E., Drugea, I. A., Duffner, L. A., Quinn, D. G., Cook, D. N., Rollins, B. J., Kovacs, E. J., and DiPietro, L. A. (2001) Wound healing in MIP-1alpha(–/–) and MCP-1(–/–) mice. *Am. J. Pathol.* **159,** 457–463

25. Siebert, H., Sachse, A., Kuziel, W. A., Maeda, N., and Bruck, W. (2000) The chemokine receptor CCR2 is involved in macrophage recruitment to the injured peripheral nervous system. *J. Neuroimmunol.* **110,** 177–185

26. Kubota, T., McTiernan, C. F., Frye, C. S., Slawson, S. E., Lemster, B. H., Koretsky, A. P., Demetris, A. J., and Feldman, A. M. (1997) Dilated cardiomyopathy in transgenic mice with cardiac-specific overexpression of tumor necrosis factor-alpha. *Circ. Res.* **81,** 627–635

27. Simeonova, P. P., Gallucci, R. M., Hulderman, T., Wilson, R., Kommineni, C., Rao, M., and Luster, M. I. (2001) The role of tumor necrosis factor-alpha in liver toxicity, inflammation, and fibrosis induced by carbon tetrachloride. *Toxicol. Appl. Pharmacol.* **177,** 112–120

28. Rathbone, C. R., Wenke, J. C., Warren, G. L., and Armstrong, R. B. (2003) Importance of satellite cells in the strength recovery after eccentric contraction-induced muscle injury. *Am. J. Physiol. Regul. Integr. Comp. Physiol.* **285(6)**, 1490–1495

29. Sabourin, L. A., and Rudnicki, M. A. (2000) The molecular regulation of myogenesis. *Clin. Genet.* **57,** 16–25

30. Ferrari, G., Cusella-De Angelis, G., Coletta, M., Paolucci, E., Stornaiuolo, A., Cossu, G., and Mavilio, F. (1998) Muscle regeneration by bone marrow-derived myogenic progenitors. *Science* **279,** 1528–1530

31. Dubois, C., Figarella-Branger, D., Pastoret, C., Rampini, C., Karpati, G., and Rougon, G. (1994) Expression of NCAM and its polysialylated isoforms during mdx mouse muscle regeneration and in vitro myogenesis. *Neuromuscul. Disord.* **4,** 171–182

32. Dickson, G., Peck, D., Moore, S. E., Barton, C. H., and Walsh, F. S. (1990) Enhanced myogenesis in NCAM-transfected mouse myoblasts. *Nature* **344,** 348–351

33. Wakelam, M. J. (1985) The fusion of myoblasts. *Biochem. J.* **228,** 1–12

34. Horsley, V., Jansen, K. M., Mills, S. T., and Pavlath, G. K. (2003) IL-4 acts as a myoblast recruitment factor during mammalian muscle growth. *Cell* **113,** 483–494

35. Mellado, M., Rodriguez-Frade, J. M., Vila-Coro, A. J., Fernandez, S., Martin de Ana, A., Jones, D. R., Toran, J. L., and Martinez, A. C. (2001) Chemokine receptor homo- or heterodimerization activates distinct signaling pathways. *EMBO J.* **20,** 2497–2507

36. Soriano, S. F., Serrano, A., Hernanz-Falcon, P., Martin de Ana, A., Monterrubio, M., Martinez, C., Rodriguez-Frade, J. M., and Mellado, M. (2003) Chemokines integrate JAK/STAT and G-protein pathways during chemotaxis and calcium flux responses. *Eur. J. Immunol.* **33,** 1328–1333

37. Anderson, M. S., and Kunkel, L. M. (1992) The molecular and biochemical basis of Duchenne muscular dystrophy. *Trends Biochem. Sci.* **17,** 289–292

38. Rudnicki, M. A., Schnegelsberg, P. N., Stead, R. H., Braun, T., Arnold, H. H., and Jaenisch, R. (1993) MyoD or Myf-5 is required for the formation of skeletal muscle. *Cell* **75,** 1351–1359

39. Hu, E., Tontonoz, P., and Spiegelman, B. M. (1995) Transdifferentiation of myoblasts by the adipogenic transcription factors PPAR gamma and C/EBP alpha. *Proc. Natl. Acad. Sci. USA* **92,** 9856–9860

Received May 28, 2004; accepted November 8, 2004.

Table 1

Histopathological grading of TA muscles at 21 days post-injury.

	Wild-type mice			CCR2–/– mice		
	Mouse #			Mouse #		
Histopathological finding	**1**	**2**	**3**	**1**	**2**	**3**
Fat infiltration	1	1	1	3.5	2	4
Fibrosis	1	1	1.5	3.5	3.5	3
Calcium deposition	1	1	1	3	3	4

Fig. 1

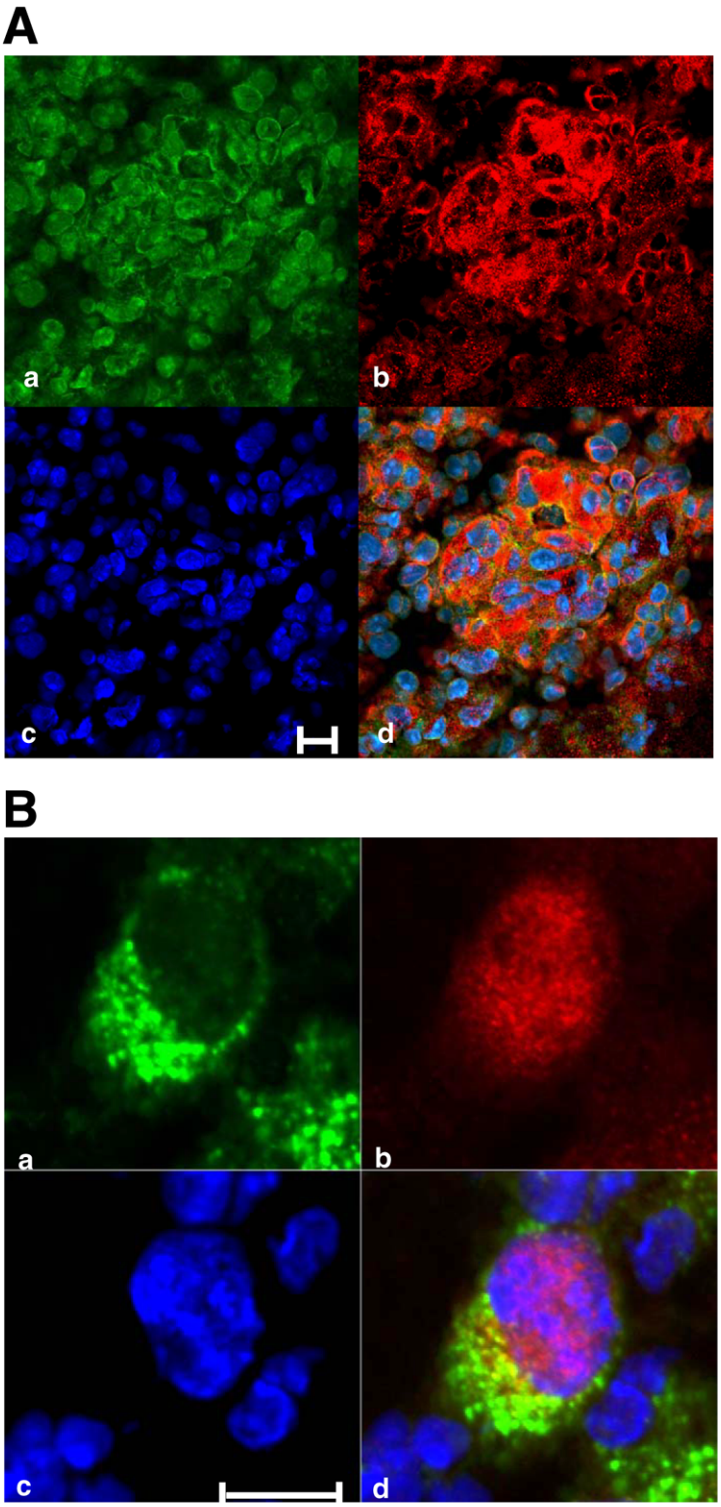

Figure 1. Immunofluorescence analysis of CCR2, Mac-1, and myogenin in TA muscle 2 days after freeze injury. Images are representative of those obtained on muscles from four wild-type mice. Nuclei were stained with DAPI and appear blue; X 640. Bars = 10 µm. Control experiments without primary antibody demonstrated that immunostaining signals observed were specific. ***A*)** CCR2-Mac-3 localization: ***a*)** image of CCR2 staining in green; ***b*)** image of Mac-3 staining in red; ***c*)** image of DAPI staining; ***d*)** a merged image showing co-localization of CCR2 and Mac-3, which produced an orange color. ***B*)** CCR2-myogenin localization: a) image of CCR2 staining (green); ***b*)** image of myogenin staining (red); ***c*)** image of DAPI staining; ***d*)** a merged image of the membrane CCR2 (green), the nuclear myogenin (red), and DAPI stainings.

Fig. 2

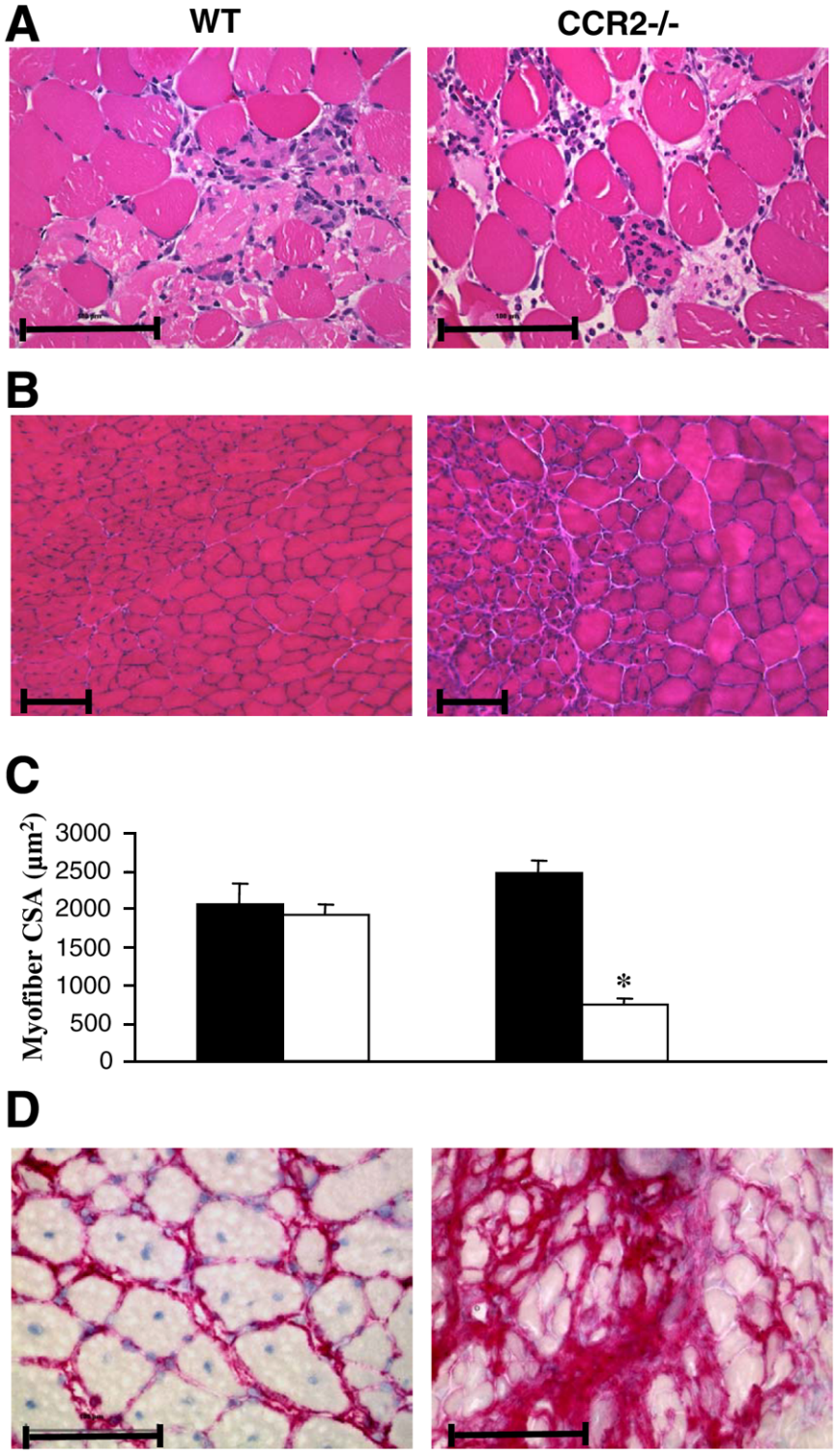

Fig. 2 (cont)

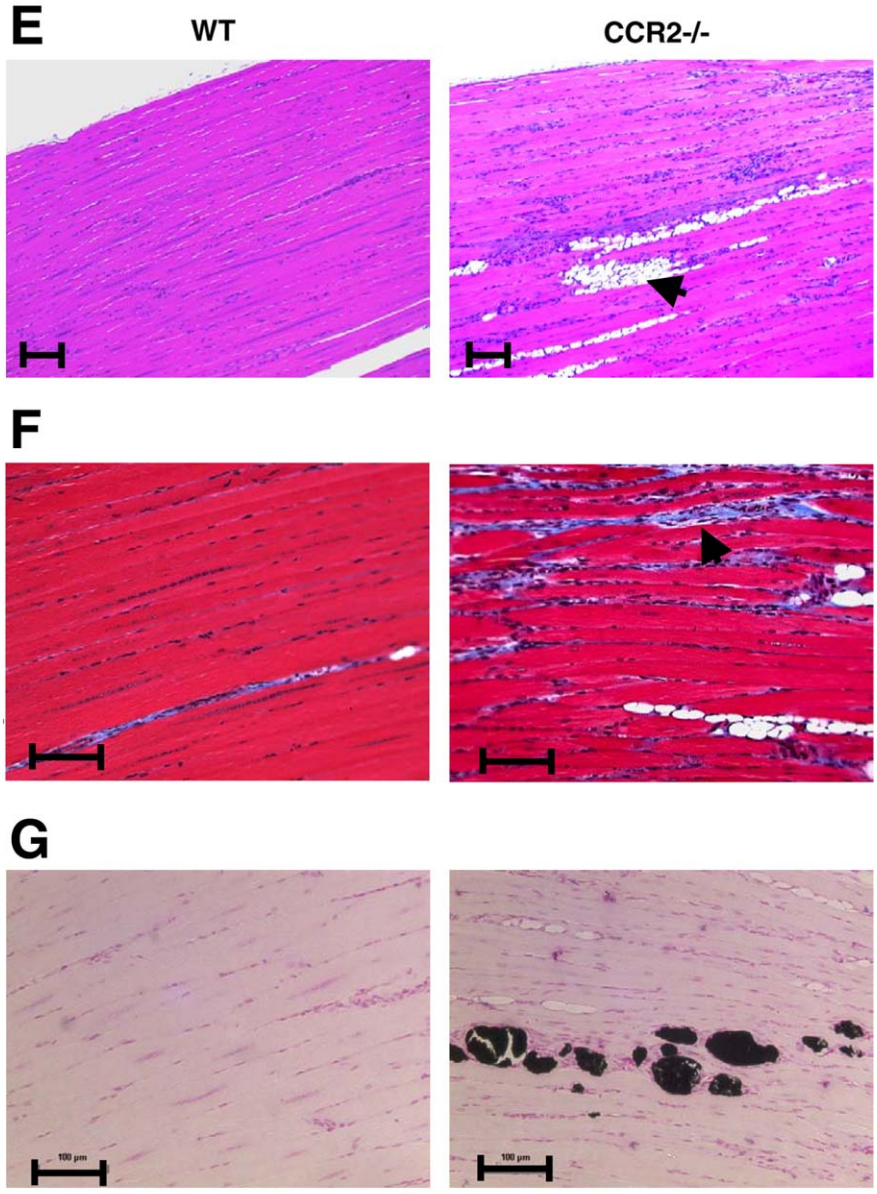

Figure 2. Microscopic appearance of TA muscle of wild-type (WT) and CCR2–/– mice at 3, 14, and 21 days following freeze injury. Images are representative of those obtained on muscles from at least four mice from each of the two groups. Bars = 100 μm. ***A*)** H&E staining of frozen transverse sections of TA muscle at three days after injury. Magnification ×400. ***B*)** H&E staining of frozen transverse sections of TA muscle at 14 days after injury. Magnification ×200. ***C*)** Average myofiber cross-sectional areas quantified for both regenerating (open bar) and uninjured myofibers (black bar) using H&E-stained histological sections obtained from muscles excised 14 day after injury [WT (*n*=5); CCR2–/– (*n*=7)]. ***D*)** ER-TR7 immunostaining on frozen transverse sections of TA muscle 14 days after injury. Magnification ×400. ***E*)** H&E staining of longitudinal sections of TA muscle 21 days post-injury (magnification ×100). The arrow indicates fat accumulation. ***F*)** Masson's trichrome staining of longitudinal sections of TA muscle 21 days post-injury (magnification ×200). The arrow indicates collagen, which stains blue. ***G*)** Van Kossa's staining of longitudinal sections of TA muscle 21 days post-injury (magnification ×200). Calcium deposits are stained dark grey.

Fig. 3

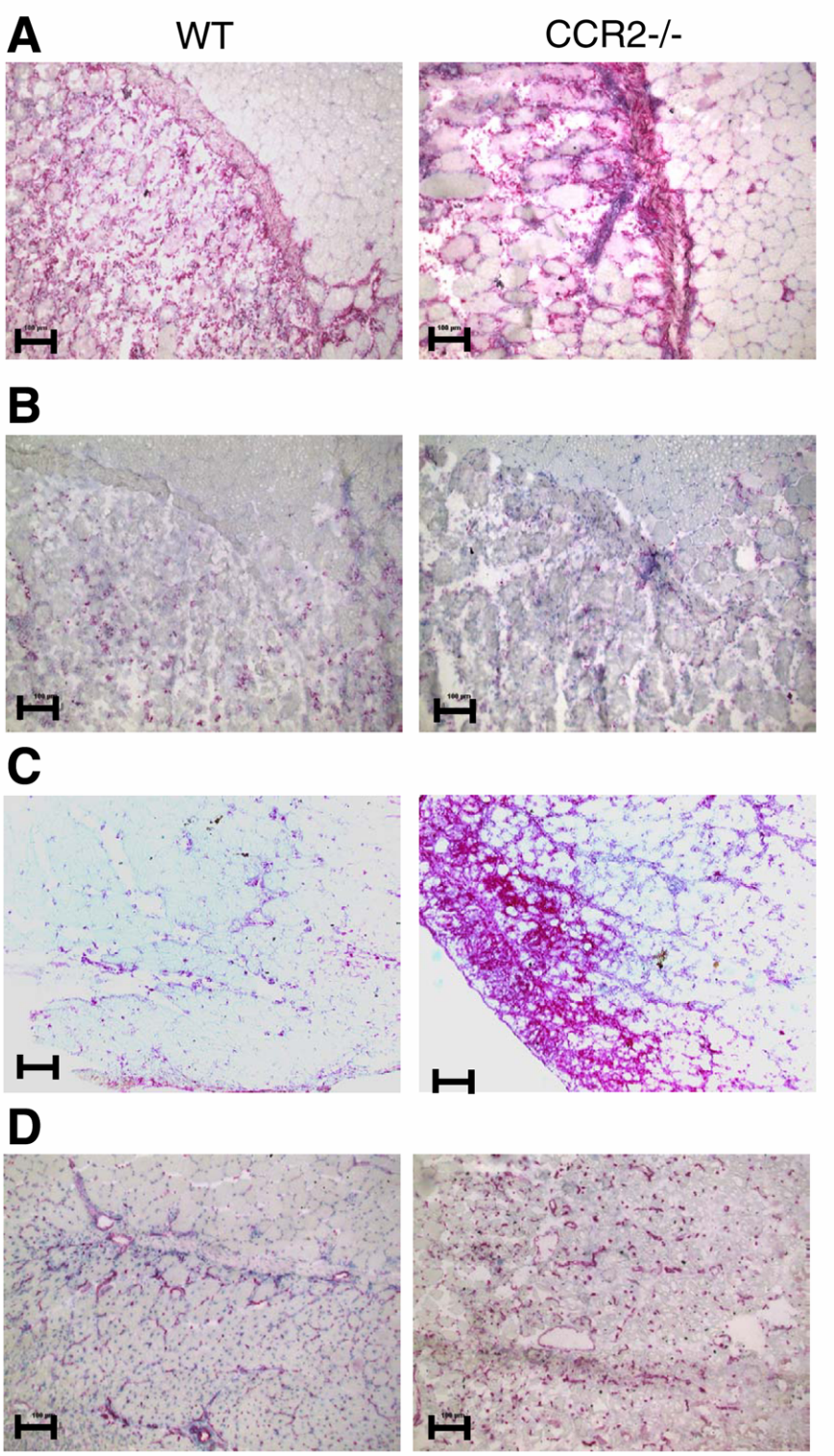

Figure 3. Microscopic evaluation for Mac-3, Gr-1, and CD31 positive cells in injured TA muscle of wild-type (WT) and CCR2–/– mice. Images are representative of those obtained on muscles of four mice from each of the two groups. Bars = 100 μm. Magnification ×100. ***A)*** Mac-3 immunostaining on frozen transverse sections of TA muscle 3 days after injury. ***B)*** Gr-1 immunostaining on frozen transverse sections of TA muscle three days after injury. ***C)*** Mac-3 immunostaining on frozen transverse sections of TA muscle 14 days after injury. ***D)*** CD31 immunostaining on frozen transverse sections of TA muscle 14 days after injury.

Fig. 4

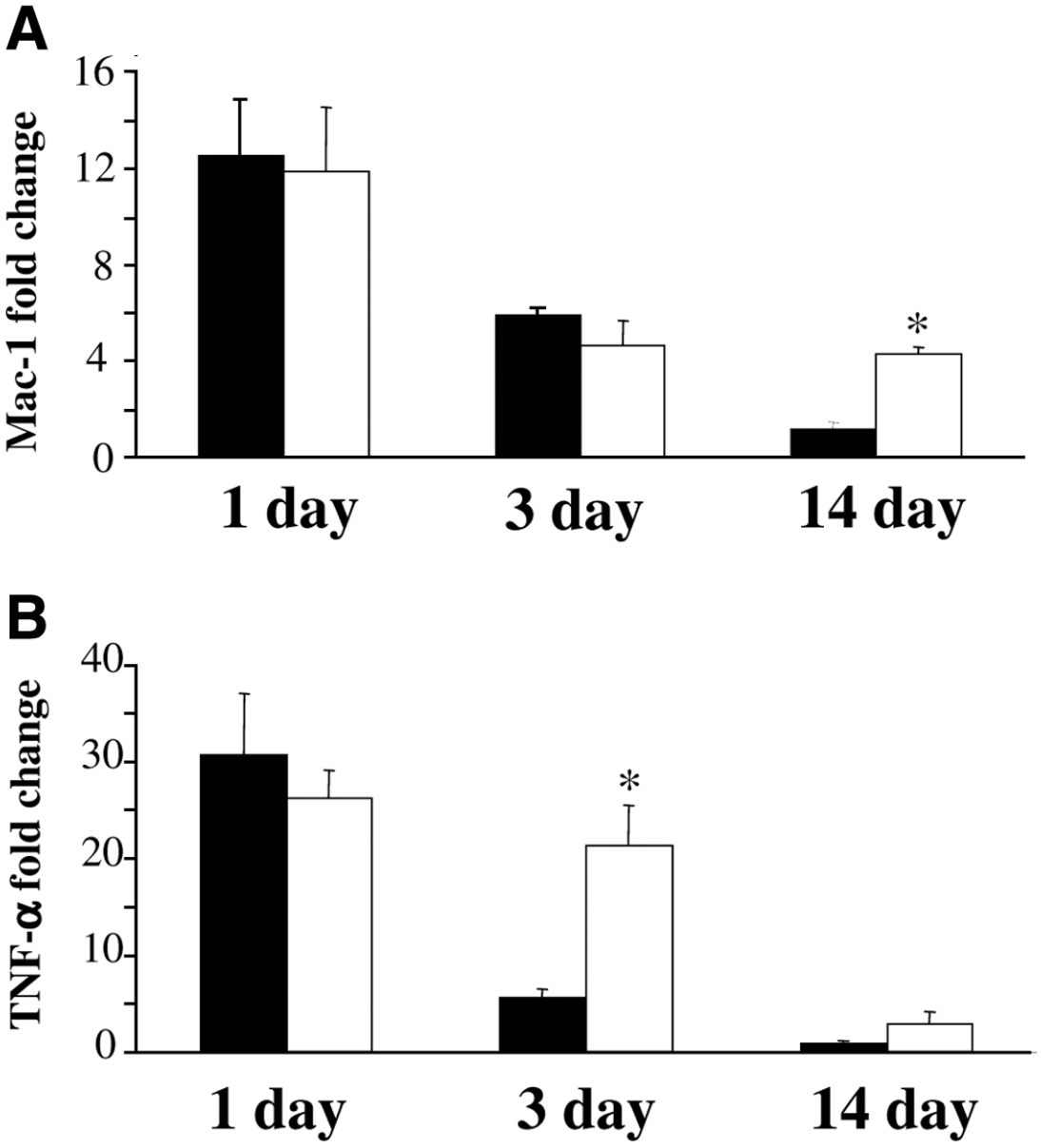

Figure 4. Time course of injury-induced Mac-1 and TNF-α expression in TA muscle of wild-type and CCR2–/– mice. Injured and uninjured (control) TA muscles were obtained from mice at the times indicated and analyzed for mRNA transcripts using real-time PCR. Expression was normalized to 28S/rRNA from the same samples and is presented as the fold-increase above control. Wild-type mice (black) and CCR2–/– mice (white). *Significantly different expression in CCR2–/– compared with wild-type mice (n=3 for days 1 and 3 and n=4 for day 14 per group, P<0.05). ***A*)** Mac-1 mRNA expression. ***B*)** TNF-α mRNA expression.

Fig. 5

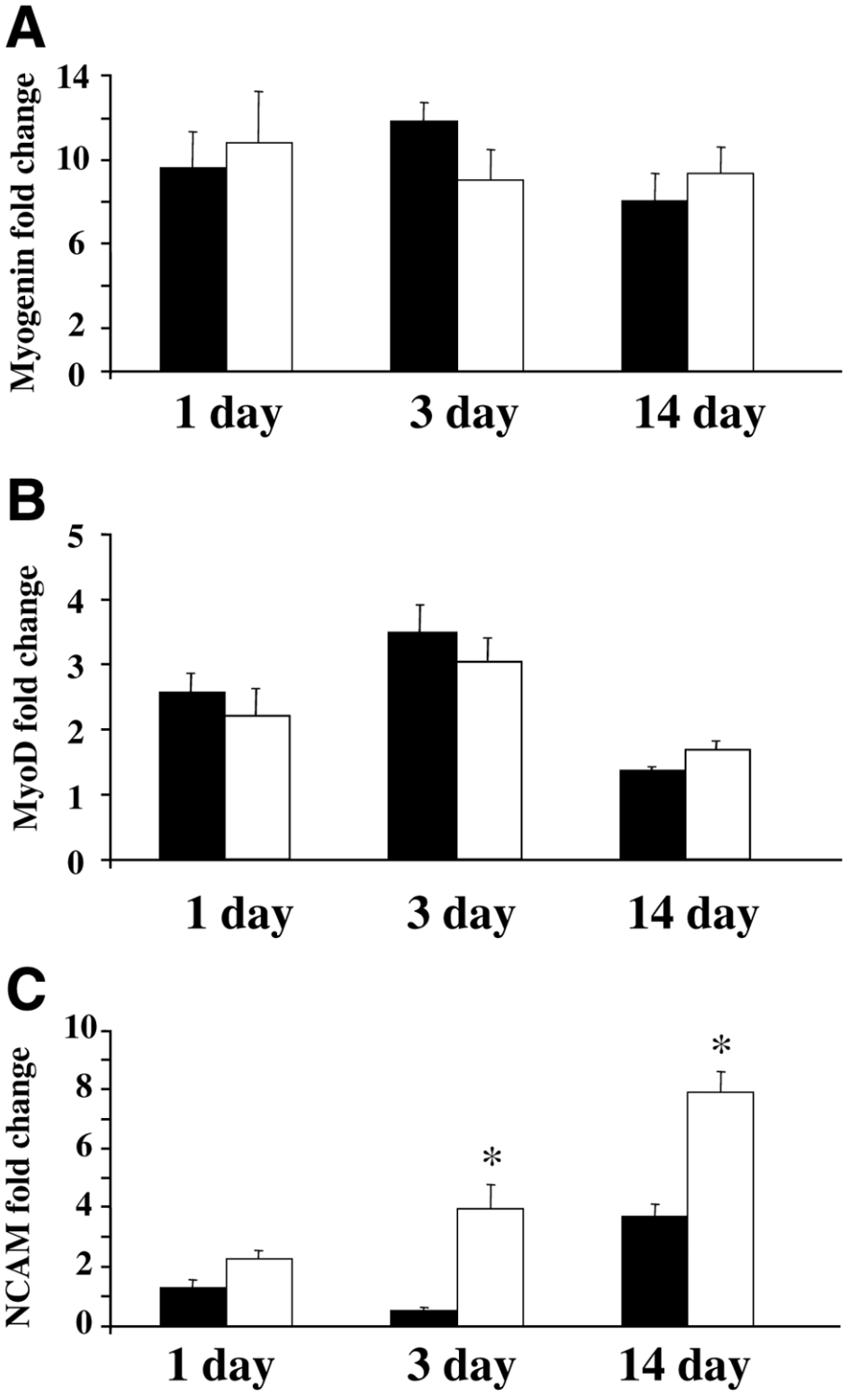

Figure 5. Time course of injury-induced myogenin, MyoD, and NCAM expression in TA muscle of wild-type and CCR2–/– mice. Injured and uninjured (control) TA muscles were obtained from mice at the times indicated and analyzed for mRNA transcripts using real-time PCR. Expression was normalized to 28S/rRNA from the same samples and is presented as the fold-increase above control. Wild-type mice (black) and CCR2–/– mice (white). *Significantly different expression in CCR2–/– compared with the wild-type mice (n=3 for days 1 and 3 and n=4 for day 14, P<0.05). ***A)*** Myogenin mRNA expression. ***B)*** MyoD mRNA. ***C)*** NCAM mRNA expression.

Fig. 6

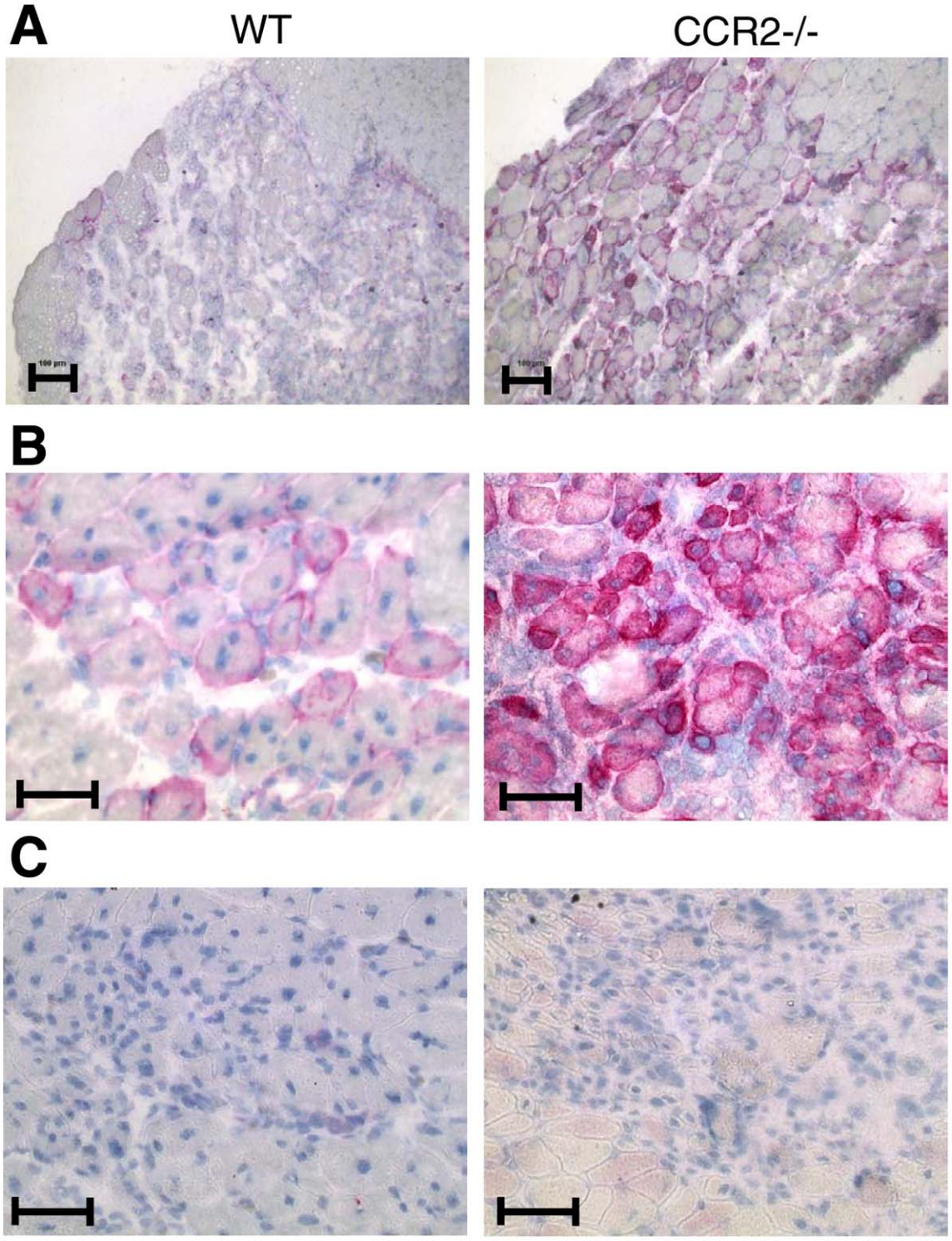

Figure 6. Microscopic evaluation of NCAM expression in injured TA muscle of wild-type (WT) and CCR2–/– mice. Images are representative of those obtained on muscles of four mice from each of the two groups. Bars = 100 μm. ***A***) NCAM immunostaining on frozen transverse sections of TA muscle 3 days after injury. Magnification ×100. ***B***) NCAM immunostaining on frozen transverse sections of TA muscle 14 days after injury. Magnification ×200. ***C***) Frozen transverse sections of TA muscle 14 days after injury treated with normal rabbit serum, which was used as a negative control for immunohistology.

Fig. 7

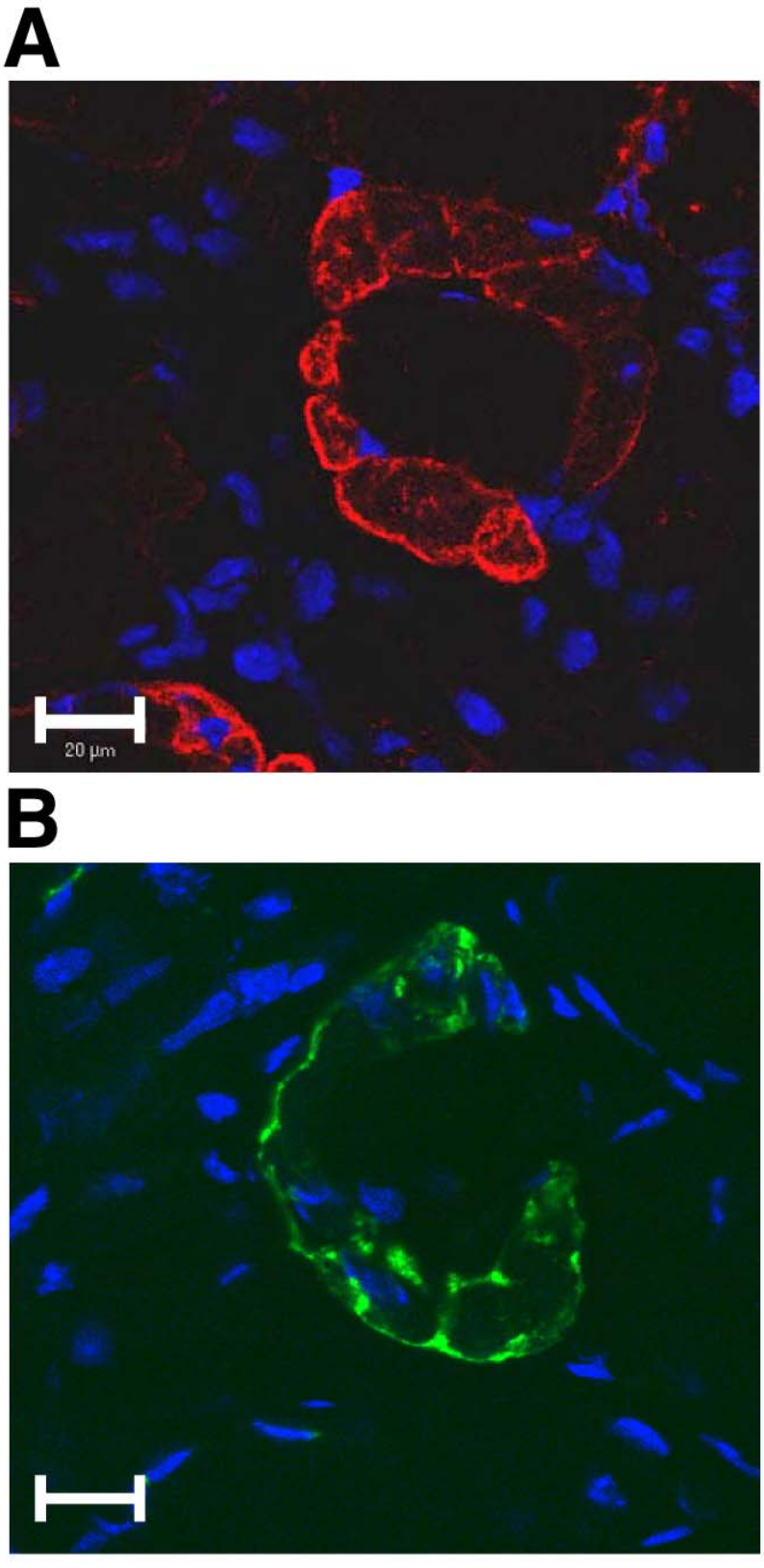

Figure 7. Immunofluorescence analysis of NCAM and desmin on serial frozen transverse sections of TA muscle from CCR2–/– mice 14 days after injury. Images are representative of those obtained on muscles from four mice. Bars = 100 µm. Nuclei were stained with DAPI and appear blue; ×640. ***A***) NCAM protein in red. ***B***) Desmin protein in green.

Fig. 8

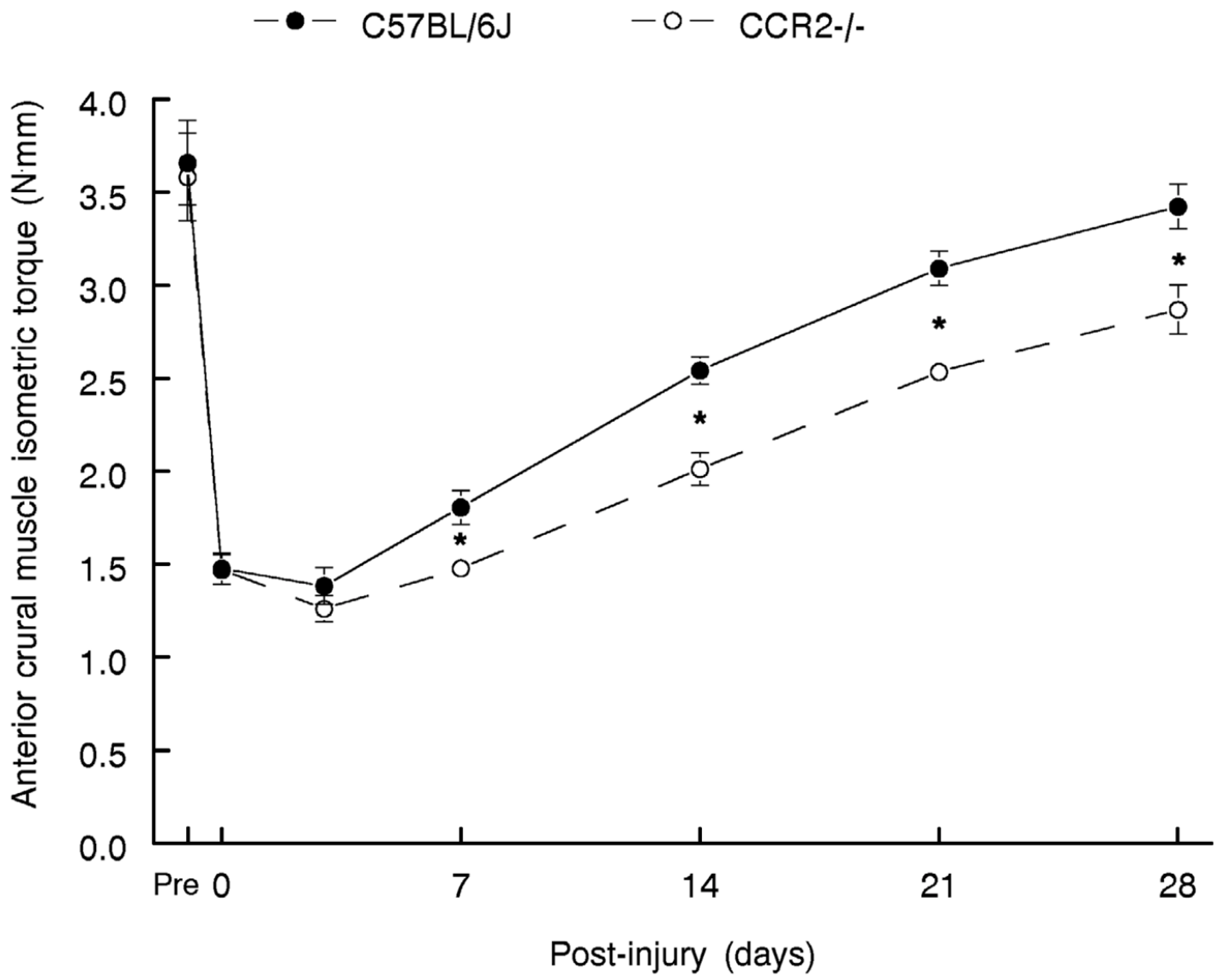

Figure 8. Time-course of the left anterior crural muscles following freeze injury in wild-type (C57BL6) and CCR2–/– mice. Anterior crural isometric torque was measured in the same group of mice before injury, immediately after injury and 5, 7, 14, 21, and 28 days after injury. Wild-type (●) and CCR2–/– (○). *Significant difference between the two groups of mice (P<0.05; n=7 mice per group).